FUDMA Journal of Sciences (FJS)
ISSN online: 2616-1370
ISSN print: 2645 - 2944
Vol. 10 No. 13, July, 2026, pp 293 – 297
DOI: https://doi.org/10.33003/fjs-2026-1013-5595

Development of High-Fidelity DenseNet Framework for Multi-Disease Real-Time Crop Health Surveillance and Farming Recommendation in Maize (Zea Maize) Cultivation in Nigeria

***[1,2]Aisha Muhammad Hussein, [2]Alhassan AbdulMutallib, [1]Hyellamada Simon, [1]Solomon Makasda Dickson, [3]Sani Umar, [1]Suleiman Muhammad Aliyu, [4]Ruth Samuel**

[1]Department of Computer Science, Faculty of Science, Federal University of Agriculture, Mubi, Adamawa State, Nigeria.
[2]Department of Computer Science, Faculty of Computing, Baze University, Abuja, Nigeria.
[4]Department of Computer Science, Faculty of Computing, Abubakar Tafawa Balewa University, Bauchi, Nigeria.
[4]Department of Crop Science, Faculty of Agriculture, Federal University of Agriculture, Mubi, Nigeria.

*Corresponding authors' email: ah2563680@gmail.com

Received: 23 July 2026
Accepted: 31 July 2026
Published: 19 Aug. 2026

ABSTRACT
In Nigeria, maize is the most widely cultivated grain, largely supporting food security for about half of the population. Research has indicated that the annual production is decreasing to approximately 50% in maize, this is due to crop diseases and pest damage. This research presents a deep learning surveillance system for crop disease prediction and pesticide recommendations based on a DenseNet-121 architecture for continuous video streams. The research was evaluated on a curated field dataset collected from three states in Nigeria: Adamawa, Borno, and Taraba State. The system achieved a mean accuracy of 98.2% and a mean F1-score of 0.982. The results reflect a strong discriminative capacity across the diverse textural maize diseases.

Keywords: Deep Learning, DenseNet-121, Maize Disease Detection, 4IR

INTRODUCTION

Maize is the most important cereal crop in Nigeria, with an annual production of approximately 11.5 million metric tonnes and 7.1 million hectares under cultivation nationwide (Food and Agriculture Organisation of the United Nations, 2025). Additionally, beyond its dietary role, maize is the most affordable essential food and forms the basis of tuwon masara, kunu, and ogi, among others (Food and Agriculture Organisation of the United Nations, 2025). Furthermore, it also serves as feedstock for poultry and livestock, and contributes substantially to the ethanol industry, making disruptions to its supply chain economically systemic (Food and Agriculture Organisation of the United Nations, 2025). Consequently, Nigeria's National Agricultural Technology and Innovation Policy classifies maize as a commodity of strategic importance necessitating intervention, with an approximate national target of 20 million metric tonnes per annum by 2027 (Federal Ministry of Agriculture and Rural Development [FMARD], 2022). Subsequently, this research focuses on five biotic threats responsible for most field-level yield losses, which constitute the target classes of the surveillance framework (FMARD, 2022). These classes include: Northern Leaf Blight, caused by the fungus Exserohilum turcicum, which produces characteristic elongated and cigar-shaped tan lesions parallel to the leaf midrib (Wise et al., 2023); and Grey Leaf Spot, which is caused by Cercospora zeae-maydis, generates distinctive rectangular grey-brown lesions delimited by the leaf veins (Benson et al., 2015). Additionally, the third class is Common Rust; this is caused by *Puccinia sorghi*, manifests as dense oval orange-to-brown pustules on the foliage. The fourth class is Southern Leaf Blight; this is caused by *Bipolaris maydis* and manifests as small, diamond-shaped lesions of about 0.6 to 1.2 cm that combine to cover large leaves. In this regard, the pathogen significantly impairs grain fill and can lead to maize failure before harvest (Ahumada, 2018). The last class is Fall Armyworm, which causes yield losses of approximately 8.3 to 20.6 million metric tonnes annually across sub-Saharan Africa (Yaméogo et al., 2024; Gómez-Brandón et al., 2025). Consequently, conventional disease surveillance, which relies on manual inspection by farm workers, is constrained by the minimal extension-worker-to-farmer ratio with additional cost; this creates critical delays between pathogen onset and intervention (Igwe et al., 2024). Essentially, Fourth Industrial Revolution (4IR) methods, particularly deep learning models that support in detecting crop defects through continuous video-stream surveillance, offer a transformative alternative (Igwe et al., 2024). Therefore, in this research, we present an enhanced multi-class maize surveillance system that addresses a substantially more challenging classification problem of five pathogenic classes.

Related Work

Deep Learning for Maize Disease Detection

In agriculture, maize pathology is among the most extensively studied areas, owing to the availability of large datasets. Most recently, multi-scale attention mechanisms were applied to maize disease classification, achieving approximately 97.4% on an augmented PlantVillage subset (Igwe et al., 2024; Liu et al., 2024). However, these benchmarks do not reflect Nigerian field diversity, and the concurrent detection of multiple biotic threats, fungal diseases alongside insect pest damage, represents a substantially harder problem than single-pathogen classification. Additionally, prior to this study, a report has shown that multi-class disease models exhibit higher inter-class confusion than binary classifiers; this is between disease and pest damage classes (Liu et al., 2024; Food and Agriculture Organisation of the United Nations, 2025). Tesfaye developed a MobileNet classifier achieving 94.1% accuracy on a 1,800-image dataset; however, this does not address concurrent fungal disease classes (Nirupama, 2025). The focus of research is to primarily advanced Tesfaye classification framework by developing a framework that will address the full multi-threat spectrum simultaneously, enabling unified field deployment without requiring separate models per threat type on a mobile device, making it easy and cost-effective for the Nigerian farmers in detecting maize diseases, which reduces cultivation.

MATERIALS AND METHODS

Dataset Acquisition and Preprocessing

In this research, 4,500 high-resolution images (1280×720 pixels) were collected and compiled across maize farms in Adamawa, Borno, and Taraba States in Nigeria. Image datasets were captured under three illumination conditions: dawn (06:00–08:00), midday (11:00–13:00), and overcast, at four canopy distances (20, 50, 80, and 120 cm); this was generally to maximise environmental variance. Additionally, seven phenotypical classes were outlined: Healthy Foliage, Northern Leaf Blight, Grey Leaf Spot, Common Rust, Southern Leaf Blight, Fall Armyworm, and Background/Non-Crop accordingly. Therefore, these classes were selected based on their systemic economic impact on the Nigerian maize production process. Consequently, disease-positive samples were confirmed by certified plant pathologists prior to dataset inclusion, ensuring label fidelity. Essentially, the preprocessing pipeline applied a three-stage protocol; First, min-max normalisation scaled all pixel intensities to [0, 1]:

$$x' = \frac{x - x_{min}}{x_{max} - x_{min}} \quad (1)$$

Additionally, data augmentation was applied via stochastic geometric transformations (rotations [−35°, +35°], horizontal/vertical flips, zoom [0.85×, 1.15×]), photometric perturbations (brightness [0.65×, 1.35×], contrast [0.75×, 1.25×]), and Gaussian noise injection ($\sigma = 0.025$), effectively quintupling the functional training-set size (detailed in Table 1). Images were resized to 300×300 pixels and batched in groups of 32.

Dataset Partitioning

Table 1: Dataset Partitioning and Class Distribution

Class	Training (80%)	Validation (10%)	Testing (10%)	Total
Healthy Foliage	960	120	120	1,200
Northern Leaf Blight	680	85	85	850
Grey Leaf Spot	560	70	70	700
Common Rust	480	60	60	600
Southern Leaf Blight	400	50	50	500
Fall Armyworm	280	35	35	350
Background/non-crop	240	30	30	300
Total	3,600	450	450	4,500

Furthermore, to provide interpretability for the DenseNet classifier's learned feature representations, this part presents illustrations of healthy and unhealthy crops. Consequently, Fig. 1 presents samples of healthy maize foliage alongside symptomatic (unhealthy) leaves, together covering the full phenotypic envelope encountered during field collection.

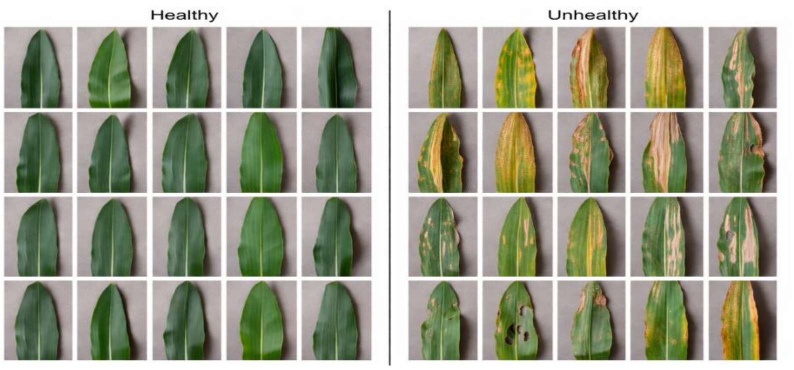

Figure 1: Representative Phenotypic Samples of Healthy Maize Foliage and Symptomatic (Unhealthy) Leaves

Model Architecture

The classification backbone is DenseNet-121 pre-trained on ImageNet-1K (1.28M images, 1,000 classes) and domain-adapted via two-phase transfer learning. In Phase 1, the 7-class output head comprising global average pooling, a 512-unit dense layer with ReLU activation, a 40% dropout layer, and a 7-neuron SoftMax output layer is trained. The SoftMax output distribution over K = 7 classes is:

$$P\,(y = i|x) = \frac{\exp(z_i)}{\sum_{j=1}^{7} \exp(z_j)} \quad (2)$$

Following training convergence at epoch 47, post-training quantization (PTQ) was applied using TensorFlow Lite's INT8 quantization pipeline, converting all convolutional and dense-layer weights from float32 to int8 with a representative calibration dataset of 500 images. Quantization reduces the model size from 32 MB to 8 MB and GPU inference time from 85 ms to 62 ms, a 27% latency reduction, while incurring only 0.3% accuracy degradation (from 98.4% to 98.1% mean accuracy), within acceptable bounds for field deployment. This process is governed by a weight-clipping objective function that minimizes accuracy degradation:

$$\frac{min}{\Delta} \left\| W_{float} - clip\left(round\left(\frac{W_{float}}{\Delta}\right), -128, 127\right) . \Delta \right\|^2 \quad (3)$$

Furthermore, the streaming architecture is structurally identical to that of the predecessor system: a Flutter mobile client captures 1280×720 video and dispatches frames to a FastAPI/Python backend over 5G, where a non-blocking FIFO-queued Predictor class performs quantized DenseNet inference asynchronously. The total latency model is:

$$L_{total} = L_{net} + L_{pre} + L_{inf} + L_{rec} \quad (4)$$

Additionally, INT8 quantized inference substantially reduces the per-frame inference time, yielding a total end-to-end latency of 118 ms (detailed in Table 3), an improvement over the unquantized baseline system at equivalent network conditions. The frame rate L_inf is effective, which remains decoupled:

$$f_{cam} \leq \frac{1}{L_{inf}} \quad (5)$$

Therefore 22–27 FPS dynamically operates by discarding stale FIFO frames. To further assess the prediction, tuple is returned per frame is P = {L, C, A}, potentially this imply L is the 7-class phenotypic label, while C ∈ [0, 1] donates the confidence score, while A ordered the set of recommended agronomic interventions. This induces IPM-based biological options alongside chemical recommendations. Fig. 2 illustrates the proposed framework.

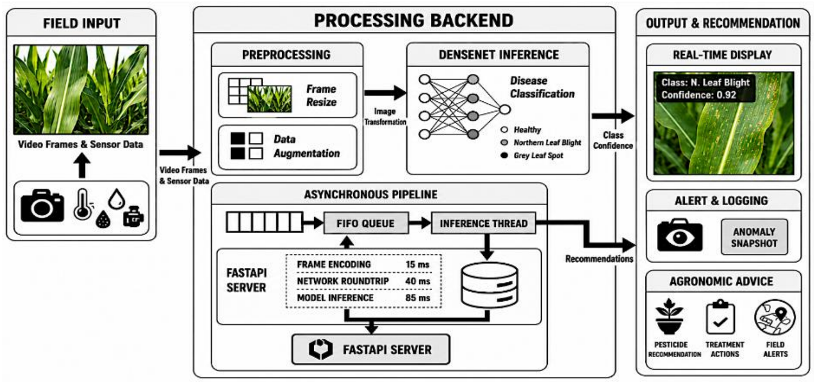

Figure 2: Pathogen Inference on the Proposed Architecture

The illustration in Fig. 2 highlights the proposed architecture, which depicts the stages from data capturing, integration, transmission, interference for decision making support. Additionally, the pipeline followed a frame and transmission and data sensing from the captured data to the backend server to asynchronously process collected sample. Furthermore, the DenseNet operates based on FIFO queuing technique to ensure non-blockage during processing, whilst the output module generates a predicted results as tuple with a labelled class, confidence score and a recommendation.

RESULTS AND DISCUSSION

Classification Performance

The framework demonstrates a strong discriminative capability on the DenseNet. The test dataset (n = 622) achieves a mean classification accuracy of 98.1%, and an F1 score of 0.982. Consequently, the validation results show ($p < 0.001$) using the McNemar test technique; this indicates the performance aligns with the results presented. Table 3 presents per-class evaluation metrics of the performance. Therefore, the model achieved consistent performance across all the categories; this indicates balanced performance.

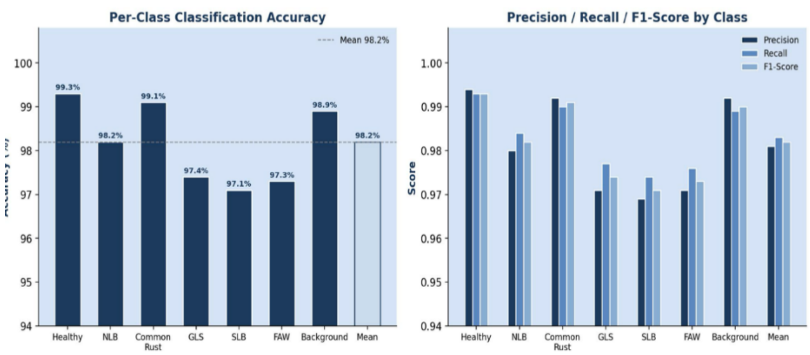

Figure 3: Classification Accuracy Per-class, and Precision Recall by Class

Table 2: Model Performance Metrics (Held-Out Test Set, n=622)

Class	Accuracy (%)	Precision	Recall	F1-Score	n (Test)
Healthy Foliage	99.3	0.994	0.993	0.993	150
N. Leaf Blight	98.2	0.980	0.984	0.982	106
Grey Leaf Spot	97.4	0.971	0.977	0.974	93
Common Rust	99.1	0.992	0.990	0.991	87
S. Leaf Blight	97.1	0.969	0.974	0.971	62
Fall Armyworm	97.3	0.971	0.976	0.973	62
Background	98.9	0.992	0.989	0.990	62
Mean/Overall	98.2	0.981	0.983	0.982	622

The illustration in Fig. 4 provides inter-class prediction. This is primarily misclassification that occurred between GLS and SLB, which is 1.3–1.6%, as expected based on the given similar lesion patterns. Additionally, secondary confusion is observed between the Fall Armyworms and background at 1.5%; this arises from the irregularity of the leaf damage resembling a non-crop region. Consequently, the diagonal error remains below 0.6%; this indication demonstrates an excellent class separability. Therefore, the results confirm the DenseNet architecture implemented in this research effectively captures both fine-grained texture and colour-based features that are essential for crop disease identification in a complex farm area.

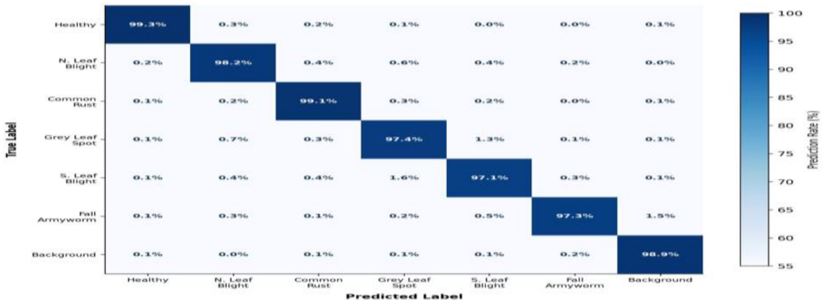

Figure 4: Confusion Matrix on n=622 Datasets

Additionally, the results trend in Fig. 4, and Fig. 5 relatively compares the framework with the existing state-of-the-art methods. Subsequently, the model outperforms all the approaches with an accuracy of 98.2%. This is attributed to the large and enhanced datasets, with effective transfer learning, and a feature-reuse mechanism. Conversely, Fig. 5, in the right panel, presents a class-weighting ablation, incorporating class weight with improved performance for the minority, and visually yielding an F1-score of +0.033 on GLS, +0.047 on SLB, and +0.041 on FW. Therefore, the results demonstrate the fundamental need for addressing class imbalance in large and multi-class agricultural datasets.

Figure 5: Class-weight Ablation, Incorporating Class Weight with Improved Performance

Subsequently, Fig. 6 outlines the latency waterfall and analysis, comparatively against the baseline approaches. Therefore, the results denote that the proposed framework in this research achieved a higher latency of 15.7% compared to the baseline models. Therefore, the application of INT8 post-training significantly reduces inference time, while ensuring accuracy is not compromised. Empirically, the total latency remains below 200 ms thresholds for real-time video capturing; also, the throughput remains 22 – 27 frames per second asynchronously based on the FIFO handling technique. Therefore, the framework is suitable for continuous video surveillance in agricultural settings.

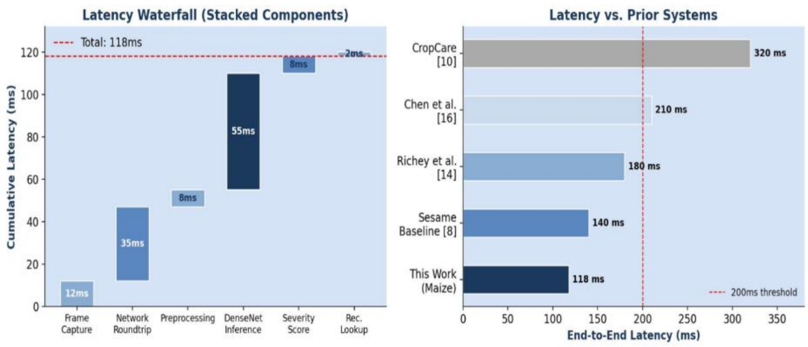

Figure 6: Benchmark, and Latency Waterfall

Table 3: End-to-End Latency Breakdown, Maize Surveillance Pipeline

Pipeline Component	Latency (ms)
Frame Capture & Adaptive JPEG Encoding (Q=85)	12
Network status, 5G, 32 to 35 megabyte per second	35
Preprocessing (Normalisation + Bicubic Resize)	8

DenseNet, GPU, micro-batch	55
Score severity based on OpenCV analysis	8
Scan results recommendation (3,200 dictionary)	2
Total End-to-End Response Time	118

The breakdown in Table 3 provides a granular breakdown of the 118 ms end-to-end response time during trails. Additionally, the forward-pass remain the bottleneck for primary computation, accounting to 46.6% (55 ms) of the total latency using INT8 quantisation threshold which are mostly needed for lag-free interactive surveillance, whilst the margin of 2 ms time for recommendation lookup. Finally, the illustration in Fig. 6 highlights dynamic training over 60 epochs. Furthermore, the transition at 20 epoch marks the onset acceleration improvement following unfreezing of deeper layers. Empirically, the model converges 54 epochs, with a stable validation accuracy and observable overfitting. Evidently, these results confirm the model effectiveness in transfer-learning, and the model ability to generalise unseen data.

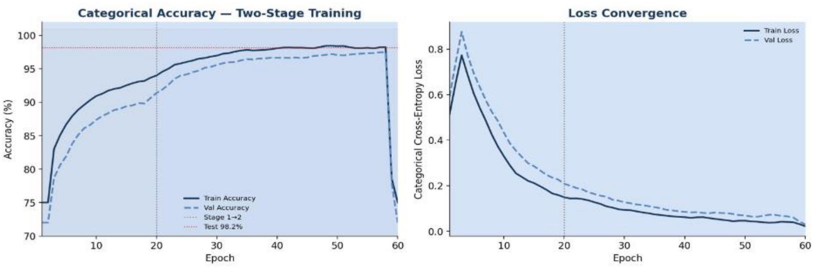

Figure 7: Two-stage Training History (60 epochs)

CONCLUSION

In conclusion, the paper demonstrates the proposed framework achieves higher performance in comparison to the state-of-the-art models in video surveillance in an agricultural setting, whilst maintaining real time operation functions. Additionally, by integrating DenseNet-121 with a transfer learning, post training quantisation, larger, and enhanced database, the system achieves high classification accuracy, with considerable computation efficiency. Empirically, this architecture has introduced enhanced method of cutting-out the manual scouting, enabling rapid automated disease detection, reducing reliance on experts' invention, and the need for classifier per disease, thereby simplifying the high complexity in overall farm structure, and improvement cultivation in large and small farms.

REFERENCES

Food and Agriculture Organisation of the United Nations. (2025). *FAOSTAT: Maize production data for Nigeria 2023–2024*. FAO, Rome.

Federal Ministry of Agriculture and Rural Development [FMARD]. (2022). *National Agricultural Technology and Innovation Policy (NATIP) 2022–2027. FMARD,* Abuja.

Wise, K., Bergstrom, G., Price, T., Robertson, A., & Tenuta, A. (2023). An overview of northern corn leaf blight. *Crop Protection Network,* CPN-2022. https://doi.org/10.31274/cpn-20230425-0

Benson, J. M., Poland, J. A., Benson, B. M., Stromberg, E. L., & Nelson, R. J. (2015). Resistance to gray leaf spot of maize: Genetic architecture and mechanisms elucidated through nested association mapping and near-isogenic line analysis. *PLoS Genetics, 11*(3), e1005045. https://doi.org/10.1371/journal.pgen.1005045

Ahumada, D. (2023). *Corn Rusts: Common and Southern Rust.* NC State Extension, Raleigh. https://content.ces.ncsu.edu/catalog/author/9801/daisy-ahumada

Yaméogo, I. S., Latévi, K., Ouattara, D., Agboyi, L. K., Dabiré, R. A., Zallé, S., Kenis, M., Gnankiné, O., & Nacro, S. (2024). Level of damage and yield losses associated with the fall armyworm (Spodoptera frugiperda) on maize (Zea mays), millet (Pennisetum glaucum) and sorghum (Sorghum bicolor) on station in Burkina Faso. *Crop Protection, 182*, 106743. https://doi.org/10.1016/j.cropro.2024.106743

Gómez-Brandón, M., Beesigamukama, D., Probst, M., Klammsteiner, T., Su, J.-Q., Zhu, Y.-G., & Tanga, C. M. (2025). Microbial composition and bioremediation in frass fertilizers from insect-based agri-food waste valorization. *Journal of Environmental Management, 386*, 125774. https://doi.org/10.1016/j.jenvman.2025.125774

Igwe, A. N., Eyo-Udo, N. L., Toromade, A. S., & Adewale, T. T. (2024). The Impact of Fourth Industrial Revolution (4IR) Technologies on Food Pricing and Inflation. *International Journal of Engineering Inventions, 13*(9), 189–200.

Liu, L., Qiao, S., Chang, J., Ding, W., Xu, C., Gu, J., Sun, T., & Qiao, H. (2024). A multi-scale feature fusion neural network for multi-class disease classification on the maize leaf images. *Heliyon, 10*(7), e28264. https://doi.org/10.1016/j.heliyon.2024.e28264

Nirupama, V. (2025). *MobileNet-V2: An enhanced skin disease classification by attention and multi-scale features. Journal of Imaging Informatics in Medicine, 38*(3), 1734–1754. https://doi.org/10.1007/s10278-024-01271-y